Control Performance of a MPPT controller with Grid Connected Wind Turbine

K. Krajangpan, B. Neammanee and S. Sirisumrannukul

Abstract— *The key issue of wind energy conversion systems is how to efficiently operate the wind turbines. This issue relies on the location where the turbines are operated. In addition, the control system with respect to machine operation and power production is essential in order to extract power from the turbines as much as possible regardless of wind speed. The control performance of a MPPT controller with a grid connected wind turbine is therefore proposed in this paper with two objectives. The first objective is to maximize the output power from the wind turbine by the maximum peak power tracking (MPPT) method. The second objective focuses on the output power from a DC generator directly coupled to the grid via a DC/AC converter or line side converter. Experiments are conducted with a 7.5kW grid connected system, using step wind speeds and a real wind speed data set from a site in a southern province of Thailand as the input of a wind simulator. The experimental results can confirm good MPPT performance and low harmonic distortion in the grid connected line side converter.*

Keywords— **Maximum peak power tracking, MPPT, wind energy conversion, grid connected.**

1. INTRODUCTION

As the impact of climate change has become public concern and the security of energy procurement is an issue, wind has become one of the fastest growing energy sources and is expected to continue growing in the electricity supply industry. The key issue of wind energy conversion systems is how to efficiently operate the wind turbines. This issue relies on the location where the turbines are operated. That is, the wind turbines should be placed where wind speed is strong and reasonably constant. In addition, the control system with respect to machine operation and power production is essential in order to extract power from the turbines as much as possible.

In general, a wind turbine is mechanically designed to produce its rating at a certain wind speed which is referred as rated wind speed. For wind speeds below the rated one, the main task of a controller is to capture the maximum power output. This task can be achieved by the maximum peak power tracking (MPPT) method.

References [1-3] propose a MPPT technique to track the maximum peak power without wind turbine characteristics. However, types of load are not considered. References [4, 5] implement controllers for grid connection via a line side converter and a transformer. The result is impressive in that active and reactive power can be directly and separately controlled with power factor near unity but the DC input source is not taken into account. It is therefore proposed in this paper a MPPT-based technique with consideration of

grid connection. The developed controller has two main objectives. [9-10]

The first objective is to maximize the output power from a wind turbine by the MPPT method. The second objective focuses on the output power from a DC generator coupled with a boost type converter to increase the DC bus voltage and directly coupled to the grid via a DC/AC converter or line side converter. Experiments are conducted with a 7.5kW grid connected system, using step wind speeds, variable wind speeds and a real wind speed data set from a site in a southern province of Thailand as the input of a wind simulator.

2. SYSTEM DESCRIPTION

A MPPT controller with a grid connected wind turbine is shown in Fig. 1. The system composed of three parts. The first part is the wind turbine coupled with a gear box and a DC generator. The wind turbine captures the energy from the wind and increases speed by the gear box to match speed of the generator. The second part is the MPPT controller composed of a power unit and control unit. The power unit consists of a boost converter which has two main functions. The first function is to amplify the DC link voltage to obtain enough voltage to match that of a 7.5 kW line side converter. The second function is to control the DC-bus output voltage for power flow control from the wind turbine to the grid to obtain the maximum peak power. The last part is a 7.5kW line side converter working as the front end of this system. The main function of the line side converter is to flow the energy production from the system to the three phase grid with a power factor of near unity. The lower part of the figure is a control unit consisting of the developed the MPPT controller, a data acquisition system and a line side converter controller. The MPPT controller receives the rotational speed form a rotary encoder, currents and voltages. The MPPT then builds a control command and sends it to the boost converter.

K. Krajangpan, B. Neammanee (corresponding author) and S. Sirisumrannukul are with Department of Electrical Engineering, King Mongkut's Institute of Technology North Bangkok 1518 Bangsue, Bangkok 10800, Thailand. Phone: (+66)2913-2500-24 Ext: 8420; Fax: (+66)2585-7350; E-mail: bln@kmutnb.ac.th.
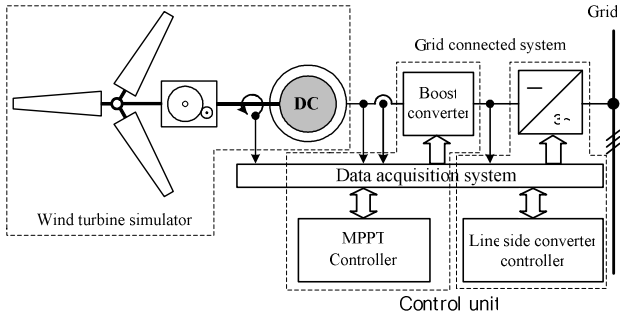
Fig. 1. MPPT controller with grid connected system for wind turbine.

2.1 Wind Turbine Characteristics

In order to describe wind turbine control schemes, a brief review of wind turbine characteristics is given here. The wind turbine characteristics are generally governed by (1) to (5).

$$T_a - T_c = J\frac{d\omega}{dt} + B\omega \tag{1}$$

$$P_a - P_c = \omega J\frac{d\omega}{dt} + B\omega^2 \tag{2}$$

$$P_a = P_W C_P(\lambda) = \frac{1}{2}\rho A v^3 C_P(\lambda) \tag{3}$$

$$\frac{1}{2}\rho A v^3 C_P(\lambda) - \eta P_{out} = \omega J\frac{d\omega}{dt} \tag{4}$$

$$\lambda = \frac{\omega R}{v} \tag{5}$$

Equation (3) reveals that the power coefficient C_P is a function of tip-speed ratio λ, which is defined by Equation (5). The C_P - λ relationship is graphically shown in Fig. 2. This figure is obtained from a real 3 kW horizontal axis wind turbine. The goal of control schemes for maximum wind power extraction is to keep wind turbine operating at their optimal tip-speed ratio, where the maximum energy conversion efficiency of wind turbine can be reached. In Figure 3, $C_P^{\max}$ is 0.4. In order to simplify the following discussion, the parameter η in (4) is assumed to be unity. Therefore, P_e is equal to P_{out}.

The power coefficient characteristic of a wind turbine has a single maximum at a specific value of the tip speed ratio. When the rotor operates at constant speed, the power coefficient will be maximum at only one wind speed. To achieve the highest annual energy capture, the value of the power coefficient must be maintained at the maximum level all the time, regardless of the wind speed [4]. For this reason, maximizing energy capture is to keep operating points at $(\lambda_0, c_P^{\max})$ of Fig. 2.

Figure 3 shows a power-rotational speed curve with seven different wind speeds ($\upsilon_1, \upsilon_2, ...,\upsilon_7$). Path A-B in the figure represents the optimum tracking path on which
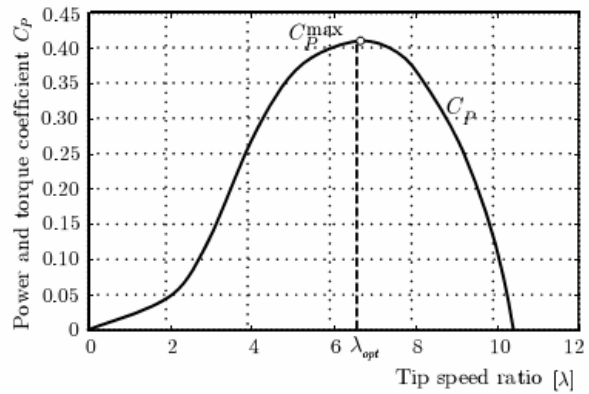
each operating point has $C_P^{\max}$ to build a rotational speed reference command, ω_{ref}, for the controller.
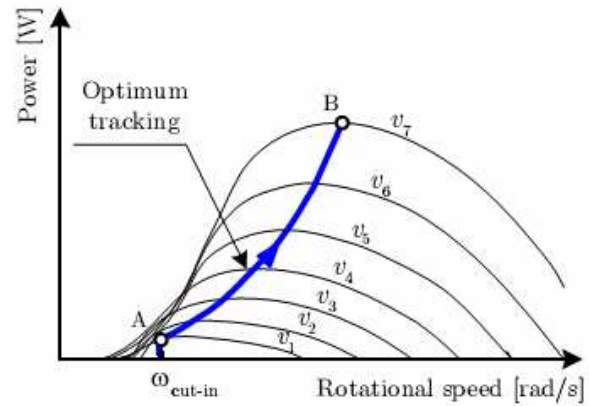
$$\omega_{ref} = \sqrt{T_a / k_T} \tag{6}$$

where

$$T_a = \frac{\rho}{2}\pi R^5 c_P^{\max}\frac{1}{\lambda_o^3}\omega_t^2 = k_T\omega_{ref}^2 \tag{7}$$

$$k_T = \frac{\rho}{2}\pi R^5 c_P^{\max}\frac{1}{\lambda_o^3} \tag{8}$$

Fig. 2. Power coefficient $C_P(\lambda)$ of real 3 kW wind turbine.

Fig. 3. Power characteristic and optimum power tracking paths.

2.2 Maximum Peak Power Tracking

Figure 4 shows typical characteristics of power and torque versus tip speed ratio of a wind turbine that needs to be controlled. The main purpose of the MPPT controller is to maintain the operating point at $P_m^{\max}$ for any wind speeds in the below rated wind speed region. At any instant of time, the operating point can be at the positive slope of the curve Fig.4 (the left hand side of the $P_m^{\max}$), at zero slope (the point where $P_m^{\max}$ occurs), or at negative slope (the right hand side of the $P_m^{\max}$). If an operating point is in the positive slope region, the controller will move it to the right to get closer to the

maximum. This can be achieved by decreasing load current, which results in an increase in rotational speed. Conversely, if the operating point lies on the right hand side of the peak, the load current has to be increased, resulting in a decrease in the rotational speed.
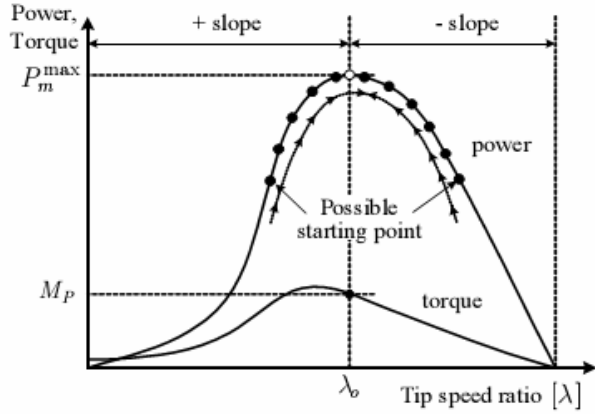

Fig. 4. MPPT process.

2.3 Line Side Converter

The line side converter links the MPPT unit with the grid. Figure 5 shows the three phase line side converter (power unit) that converts AC voltage to DC voltage by a space vector PWM converter. The per phase voltage equation can be written as in (9)-(11). [4-8]
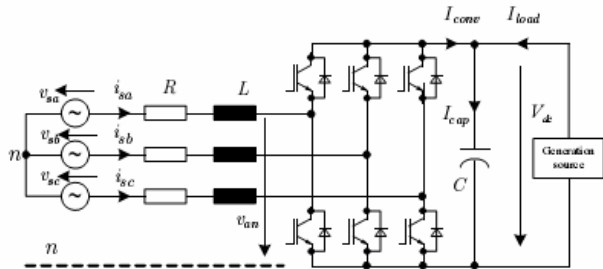

Fig. 5. Line side converter (power unit).

$$v_{sa} = Ri_{sa} + L\frac{di_{sa}}{dt} + v_{an} \tag{9}$$

$$v_{sb} = Ri_{sb} + L\frac{di_{sb}}{dt} + v_{bn} \tag{10}$$

$$v_{sc} = Ri_{sc} + L\frac{di_{sc}}{dt} + v_{cn} \tag{11}$$

Transforming (9)-(11) in three phases in stationary reference frame to two phase synchronous reference frame (*d*-, *q*-axis) gives:

$$v_{sd} = (Ls + R)i_{sd} - \omega L i_{sq} + v_{dn} \tag{12}$$

$$v_{sq} = (Ls + R)i_{sq} + \omega L i_{sd} + v_{qn} \tag{13}$$

For the balance three phase system,

$$v_{sd} = V_m \text{ and } v_{sq} = 0 \tag{14}$$

The converter power, P_{conv}, and current, i_{conv}, can be calculated by (15) and (16) [3].

$$P_{conv} = \frac{3}{2}\left(v_{sd}i_{sd} + v_{sq}i_{sq}\right) \tag{15}$$

$$I_{conv} = \frac{P_{conv}}{V_{dc}^*} = \frac{3}{2}\frac{\left(v_{sd}i_{sd} + v_{sq}i_{sq}\right)}{V_{dc}^*} \tag{16}$$

The capacitor current, I_{cap}, and DC bus voltage, V_{dc}, can be calculated by (17) and (18).

$$I_{cap} = I_{conv} - I_{load} \tag{17}$$

$$V_{dc} = \frac{1}{Cs}\int I_{cap}dt \tag{18}$$

With the transformation of (12)-(18) into s-domain, a block diagram in *d*-, *q*-axis reference frame can be constructed as shown in the right hand side of Fig. 6 (rectifying model). It is clear that there is voltage cross coupling between v_{dn} and v_{qn}. To have independent control of V_{dc}, the coupling voltage should be compensated by a controller [4-5].
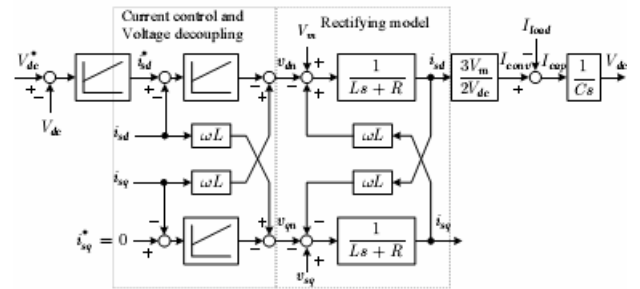

Fig. 6. Line side converter with voltage decoupling control.

3. CONTROL BLOCK DIAGRAM

3.1 MPPT Controller with Grid Connected Wind Turbine

Figure 7 shows the power circuit connection of this system composed of the MPPT controller with the boost converter, the line side converter and the grid. The MPPT controller receives the rotational speed, w, generator voltage, V_g, and current, i_g, to calculate a change of rotational speed to obtain the maximum output power. The MPPT controller increase or decrease the speed by decreasing or increasing the duty cycle of the full-bridge converter. Accordingly, the output voltage will decrease/increase. The voltage will be stepped up by the transformer T_1 and rectified by the full bridge and the capacitor C_1 in order to match the voltage of the line side converter in the next part. If the output voltage is higher than a specified dc bus voltage (550V), the energy will flow to the grid passing through the line side converter (higher voltage and therefore higher energy is flowing to the grid). The energy will stop flowing when the boosted voltage is equal to or less than the specified value.
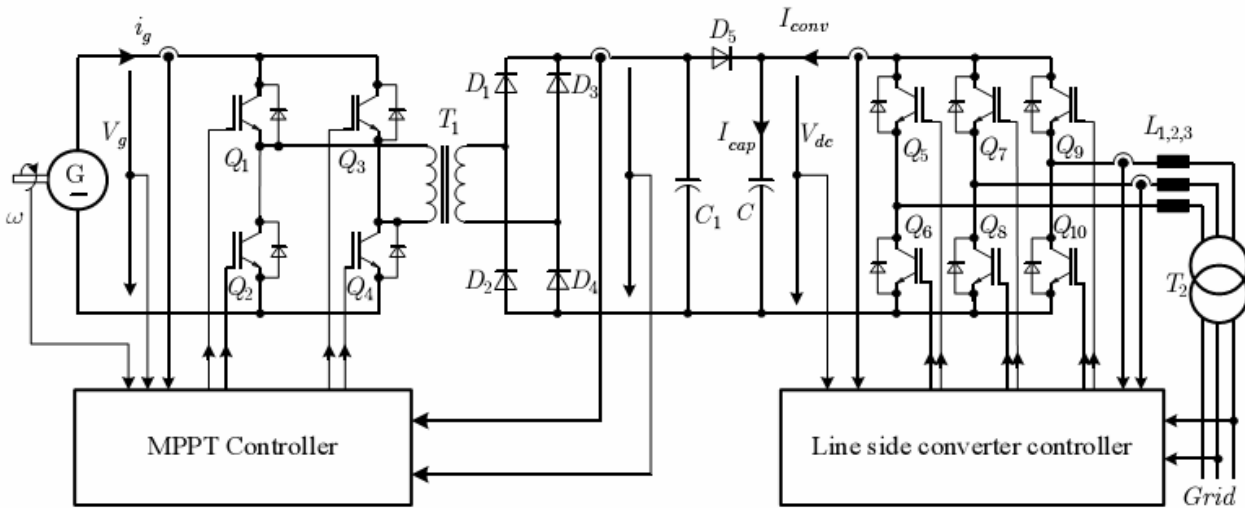
3.2 MPPT Controller

The MPPT controller in the lower left corner of Fig. 7 can be explained in more detail as shown in the block diagram in Fig. 8. The top part of the diagram which is enclosed in the dotted line represents the MPPT controller built from (19) and (20). The MPPT controller receives the generator current, voltage and rotational speed from the plant as inputs and uses them to calculate the slope of the power-speed curve. The rate of change of power is compared with the reference (zero rate of change of power). The error is multiplied by the dc gain, M, to generate the current reference for the PI controller of the plant control system.

The tracking process can be achieved by decreasing load current, which results in an increase in the rotational speed. On the other hand, if the operating point lies at the right hand side of the peak power point, the load current has to be increased, resulting in the decrease in the rotational speed. The step increase or decrease of load current is made with reference to the relative position with P_m^{max}. This tracking methodology is called the perturbation and observation method (P&O). The current reference is calculated from

$$i_{bref}[(k+1)T_s] = i_{bref}[(k)T_s] + M \frac{\Delta p[(k)T_s]}{\Delta \omega_t[(k)T_s]} \qquad (19)$$

The slope of instantaneous power curve is given by

$$slope = \frac{\Delta p[(k)T_s]}{\Delta \omega_t[(k)T_s]} \qquad (20)$$

The current reference is updated by the MPPT controller at every time step T_s. The above mentioned actions bring the operating point towards P_m^{max} by step-by-step increasing or decreasing the rotational speed.

3.1 Line Side Converter Controller

In Fig. 6, the voltage cross coupling is compensated by feeding i_{sd} and i_{sq} with gain wL on the left hand side of Fig.6. After the voltage is decoupled, the DC bus voltage

is controlled by two loops: current and voltage loops. The current i_{sq} does not affect the bus voltage and therefore it is not used and the value of i_{sq} is set to zero.
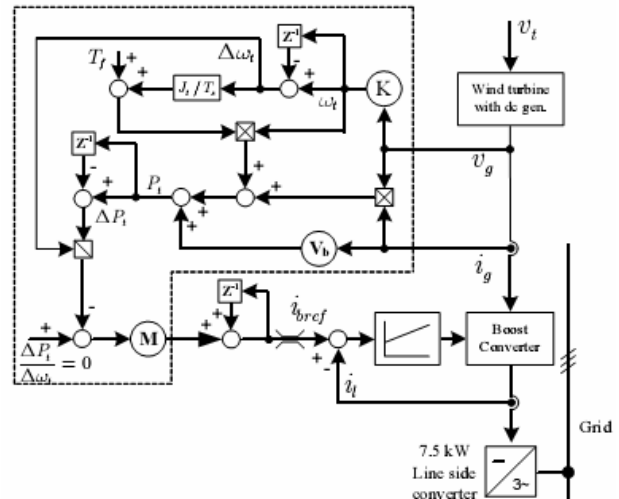

Fig. 8. Block diagram of the MPPT control system with grid connected wind turbine.

The line side converter controller in the lower right corner of Fig. 7 can be explained in more detail as shown in the block diagram of Fig. 9. The controller of the line side converter is controlled in the d-, q-axis reference frame. The transformation between three phases and the d-, q-axis requires an angle of phase voltage. A phase locked loop (PLL) to calculate the angle of phase voltage, θ^*, is shown in Fig. 4 [6]. The PLL is composed of voltage transformation, sine and cosine calculation and PI controller. The parameter θ^* in the transformation is obtained by integrating frequency command ω^*. If the frequency is identical to the grid frequency, the voltages v_{sd} and v_{sq} become DC values, depending on the angle θ^*. A PI regulator is used to obtain that value of ω^*, which drives the feedback voltage v_{sq} to the command value v_{sq}^*. The magnitude of the controlled quantity v_{sq} determines the phase difference between the utility

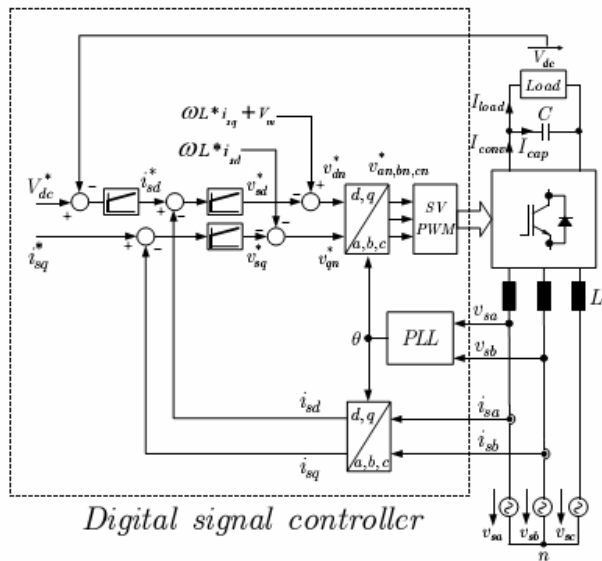voltages and $\sin(\theta^*)$ or $\cos(\theta^*)$. This system sets $v_{sq}^* = 0$.

Fig. 9. Line side converter control block diagram.

4   CASE STUDY

Test System

There are two main parts of the test system shown in Fig. 10: 1) a wind turbine simulator [11] on the left hand side of Fig. 10 and 2) a purposed wind turbine controller on the right side of Fig. 10. The data of the wind turbine is provided in appendix. The first part is given in detail in [11] and not repeated here because of limited space. The proposed controller consists of a boost converter connected between a generator line side converter and the grid (a load), voltage and current sensors, a data acquisition unit and a DSC controller. The controller board uses a high performance 16 bits dsPIC30f6010 combining the advantage of a high performance 16-bit microcontroller (MCU) and a high computation speed digital signal processors. Software was implemented in this DSC and performed to link a personal computer via two RS232 ports: one for transferring wind speed data to the DSC board and the other for sending parameters (e.g., P_e, i_g, v_g, w_g) to the computer.
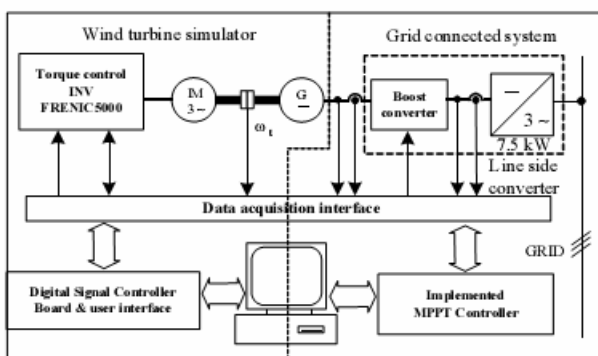

Fig.10. The test system.

4.1 MPPT Control Trajectory with Step Wind Speed

The experiment began by starting up the wind turbine simulator at a wind speed of 4.5m/s to verify the tracking performance of the developed MPPT controller. The controller would try to track the maximum peak power as fast as possible by reducing P_e and thus resulting in an increase in w_t. When an operating point with the maximum power was found (i.e., $dP_t / dw_t = 0$), the controller tried to keep staying at that point.

The objective of this experiment was to track the maximum output power of the turbine. The wind simulator was started at a wind speed of 4m/s, stepped up to 4.5, 5 and 6 m/s respectively and run until steady state. The MPPT controller would capture maximum powers of 260, 420, 600 and 900 W respectively. The power versus rotational speed is shown in Fig. 11 and the output torque versus rotational speed is shown in Fig. 12. It is clearly seen that at the maximum output power, the aerodynamic torque are not maximum. Figure 13 (a) shows the relationship between c_P and time obtained from the experiment. It can be seen from the figure that in this case, the MPPT controller can manage to keep c_P at 0.4 for the four step wind speeds. The power for each wind speed is shown in Figure 13 (b).
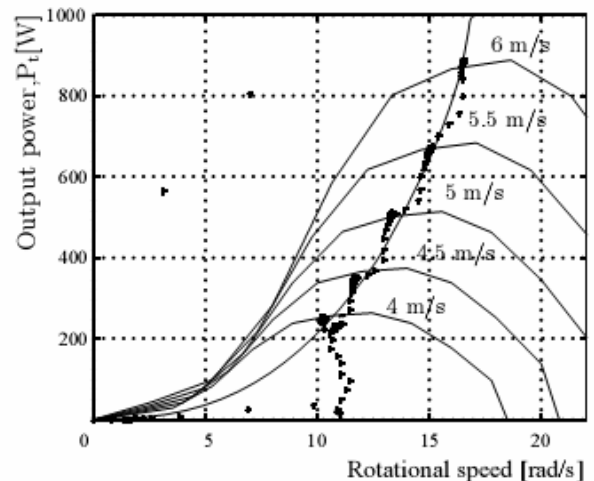

Fig. 11. The control trajectory of MPPT controller in the power versus rotational speed with various wind speed.

MPPT Control Trajectory with Real Wind Speed Data

This experiment used a real wind speed data set obtained from a site in Trung, a province situated in the southern part of Thailand, as the input of the wind turbine simulator. The data are classified as variable wind speed. Figure 14 shows the real wind speed data and the output power controlled by the MPPT controller. Figure 15 plots the control trajectory of the output power versus rotational speed. It is clear that the MPPT controller can track the maximum with the variable wind speed.

Grid Connect Converter

The line side converter is tested with the condition that the power factor of the line side is kept at unity. A

conventional PI controller is implemented. Figure 16 shows the dynamic performance of the line side converter, the DC link voltage and currents i_{sd} and i_{sq} response for step load disturbance rejection. It can be seen that, the line side converter controller decrease i_{sd} to regulate the DC link voltage with low percentage of overshoot.
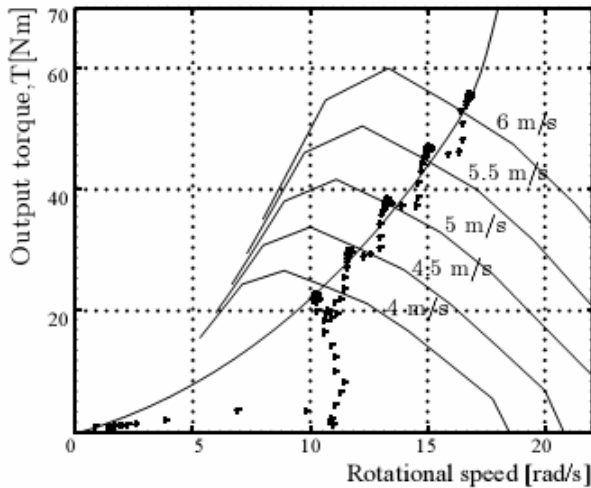

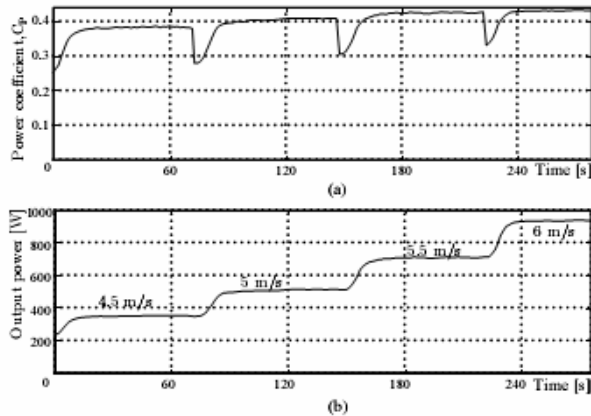**Fig. 12. The control trajectory of MPPT controller in the torque versus rotational speed with various wind speed.**

Fig. 13. Output power and power coefficient with time.

Figure 17 shows the phase voltage and phase current of the grid connected line side converter. It can be seen that voltage and current are 180 degree out of phase. Therefore, the power flow from the wind turbine to grid with a phase current near sinusoidal with low harmonic distortion.

CONCLUSION

The control performance of the MPPT controller is verified by the developed 7.5 kW wind turbine simulator. The MPPT controller and line side converter are implemented on a dsPIC 30f6010 digital signal controller board with C language. Experiments are set up for testing the control performance of the MPPT controller and line side converter in inverting modes with grid connection. The experimental results confirm that the system can track the maximum output power with

various wind speeds and can regulate the DC bus voltage under nonlinear load generated from the wind turbine with nearly sinusoidal line side current, near-unity power factor and low harmonic distortion. The advantages of the MPPT controller are that it does not require any knowledge of a machine model, and turbine characteristic curves. The developed MPPT controller is useful in case of, for example, dirty blades, varying local air flow effects or blades with non-optimum pitch angles. Although these factors change the characteristics of the wind turbine, they do not affect the proposed control strategy.
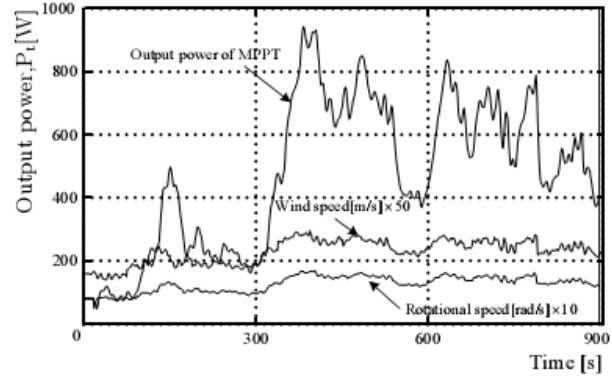

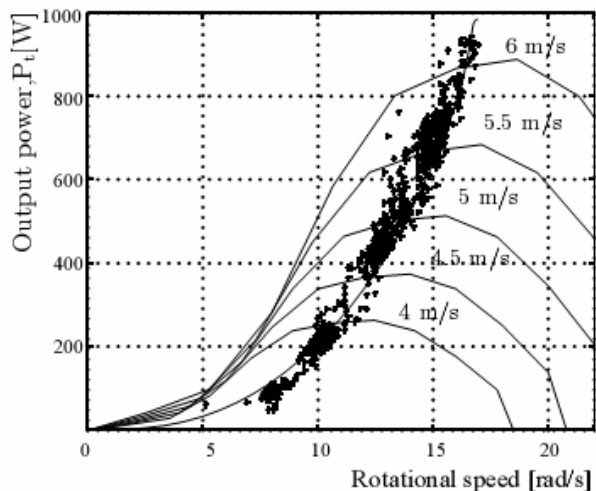**Fig. 14. Real wind speed and the corresponded output power.**

Fig. 15. The control trajectory of MPPT controller in the power versus rotational speed with various wind speed.

NOMENCLATURE

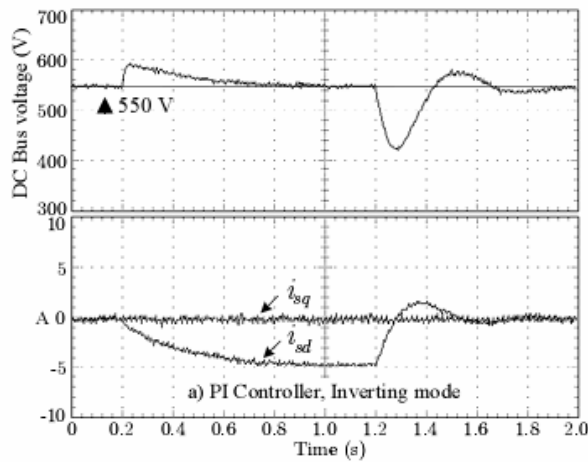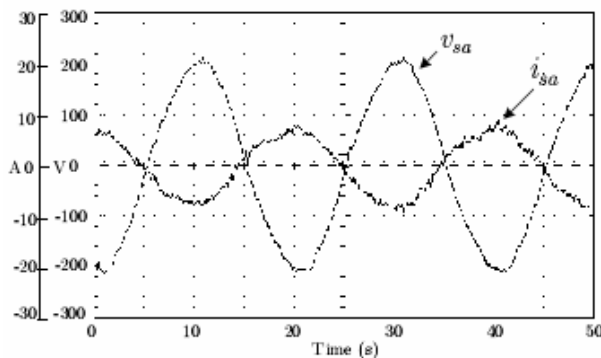|	
T_a	wind turbine mechanical torque;
T_e	load torque;
J	turbine moment of inertia;

Fig.16. DC bus voltage with step wind speed.

Fig. 17. Line voltage, v_{sa} and current, i_{sa} in inverting mode.

ω	turbine angular speed;
B	friction
P_a	turbine mechanical power;
P_W	wind power
P_{out}	system output power;
P_c	turbine load power;
v	wind speed
A	sweeping area of turbine rotor
C_P	turbine performance coefficient;
λ	tip-speed ratio;
R	maximum radius of the turbine rotor;
η	efficiency of the generator-inverter set
ρ	air density
k_T	Torque constant
v_{sd}, v_{sq}	d- and q-axis voltages
i_{sd}, i_{sq}	d- and q-axis currents
V_{dc}	dc bus voltage
I_{load}	Load current
I_{cap}	Capacitor current
I_{conv}	converter current
P_{conv}	converter power
V_m	Peak voltage
k	constant which depends on the transformation used

R,	input filter resistance
L_1, L_2, L_3	inductance
$Q_1, Q_2, ..$	IGBT
T_1, T_2	transformer
$D_1, D_2, ..$	diode
V_g	Generator voltage
i_g	Generator current
v_t	Wind speed
V_b	Brush voltage
P_{loss}	losses in the converter
i_{load}	load current connected to the DC link capacitor
$i_{bref}(k)$	reference current at k
M	step size
T_s	update time

REFERENCES

[1] Neammanee, B., Chatratana, S. 2006. Maximum Peak Power Tracking Control for the new Small Twisted H-Rotor Wind Turbine. In *Proc. of International Conference on Energy for Sustainable Development: Issues and prospect for Asia*, Phuket, Thailand, 1-3 Mar.

[2] Koutroulis E., Kalaitzakis K., Voulgaris N.C. 2001. Development of a Microcontroller-Based, Photovoltaic Maximum power Point Tracking Control System. *IEEE Trans. Power Electronics*, 16: 46-54.

[3] Huynh, P., Cho, B.H. 1996. Design and analysis of a Microprocessor-Controlled Peak-power-Tracking System. *IEEE Trans. Aerospace and Electronic Systems*, 32(1): 182 – 190.

[4] Sudmee, W., Neammanee, B. 2007. Control and Implementation of Line Side Converter for Doubly Fed Induction Generator of Wind Turbine. *International Conference on Electrical Engineering Electronics, Computer, Telecommunications and Information Technology (ECTI)*, Chiang Rai, Thailand, 9-12 May, 249-252.

[5] Dixon. J.W., Ooi. B.T. 1988. Indirect current control of a unity power factor sinusoidal boost type three-phase rectifier. *IEEE Trans. Industrial Electronic*, 35(4): 508-515.

[6] Rim, C.T., Choi, N.S., Cho G.C., Cho, G.H. 1994. A complete DC and AC Analysis of Three-phase Current PWM Rectifier Using d-q Transformation. *IEEE Trans. Power Electronics,* 9(4): 390-396.

[7] Lee, D.-C. 2000. Advanced nonlinear control of three-phase PWM rectifiers. *IEE Proc. on Electric Power Appl.*, 147(5): 361-366.

[8] Kaura, V., Blasko, V. 1997. Operation of a Phase Locked Loop System under Distorted Utility Condition. *IEEE Trans. Industry Application*, 33(1): 58-63.

[9] Carrasco, J.M., Franquelo, L.G., Bialasiewicz, J.T. Galvan, E., PortilloGuisado, R.C., Prats, M.A.M., Leon. J.I., Moreno-Alfonso, N. 2006. Power-Electronic Systems for Grid Integration of

Renewable Energy Sources: A Survey. *IEEE Trans. Industry Electronics*, 53(4): 1002-1016.

[10] Schulz, D., Fabis, R., Hanitsch, R.E. 2003. A Three Phase Power Electronic Converter for Grid Interration of Distributed Generation. *Power Tech Conference Proceedings*, 23-26 June, Bologna, Italy, 1002-1016.

[11] Neammanee, B., Sirisumrannukul, S., Chatratana, S. 2007. Development of a Wind Turbine Simulator for Wind Generator Testing. *International Energy Journal*, 21-28.

APPENDIX

This is the wind turbine simulator parameters

Wind turbine type	Horizontal
Number of blades	3 blades
Maximum power coefficient	0.40
Optimum tip speed ratio	5
Blade radius	2.25 m
Gear ratio	8
Turbine moment of inertia	11.3